

## Amorphous Silicon X-Ray Detectors

M. Hoheisel<sup>\*</sup>, M. Arques<sup>+#</sup>, J. Chabbal<sup>+</sup>, C. Chaussat<sup>+</sup>, T. Ducourant<sup>+</sup>,  
L. Fritsch<sup>+</sup>, G. Hahm<sup>\*</sup>, H. Horbaschek<sup>\*</sup>, J. Michailos<sup>+</sup>, R. Schulz<sup>\*</sup>,  
M. Spahn<sup>\*</sup>, V. Spinnler<sup>+</sup>, and G. Vieux<sup>+</sup>

<sup>\*</sup> Siemens AG, Medical Engineering, Basic Development  
P.O.Box 3260, 91050 Erlangen, Germany

<sup>+</sup> Thomson Tubes Electroniques, 38430 Moirans, France

### ABSTRACT

An X-ray detector consisting of a CsI scintillator coupled to an amorphous silicon photodiode matrix was developed. Design and performance of this  $20 \times 20 \text{ cm}^2$  sized device are presented. Its outstanding performance represents a first step towards the goal of replacing existing fluoroscopic or radiographic X-ray systems for medical diagnosis.

### 1. Introduction

In the field of medical diagnosis, systems are required which convert X-ray images, i.e. the spatial distribution of X-ray dose after passing the body to be examined, into visible images. There are analog and digital systems available, also systems for single images or for image sequences. Even acquisition in real-time is feasible. The following contribution will restrict itself to projection systems, excluding computed tomography.

The traditional analog system is the film-screen combination, which yields single images. A film is sandwiched between two scintillating screens. The latter convert X-rays into visible light which exposes the film.

Image sequences can be taken by a film camera from the output screen of an X-ray image intensifier (XRII).

Single digital images can be obtained by a storage phosphor plate which is read out by a laser scan or by an electrostatically probed selenium drum<sup>1</sup>. The combination of an XRII with a TV camera enables real-time imaging.

Conventional systems suffer from several drawbacks: the X-ray dose required is still too high (from this follows a demand for a higher DQE (Detective Quantum Efficiency)), the spatial resolution especially over large areas could be better, geometrical distortions disturb the periphery of the image in the case of XRIIs, and detector weight and bulky geometrical dimensions rule out a lean system.

Therefore, solid state detectors based on amorphous silicon (a-Si) are under development<sup>2-5</sup>. The operating principle is fairly simple: an input screen

---

# permanent address: LETI, Grenoble, France

consisting of CsI as a scintillator converts X-ray quanta into visible photons. These photons are transformed to charges by a matrix of a-Si photodiodes and subsequently read out.

On the contrary, the conventional XRII-TV chain involves many conversion steps (Fig. 1): absorbed X-ray quanta are converted first to visible photons, then to electrons. They are accelerated towards the output screen where they generate visible light. The light is projected via an optical system on a video camera where the photons are again transformed to charge carriers which are scanned by the electron beam.

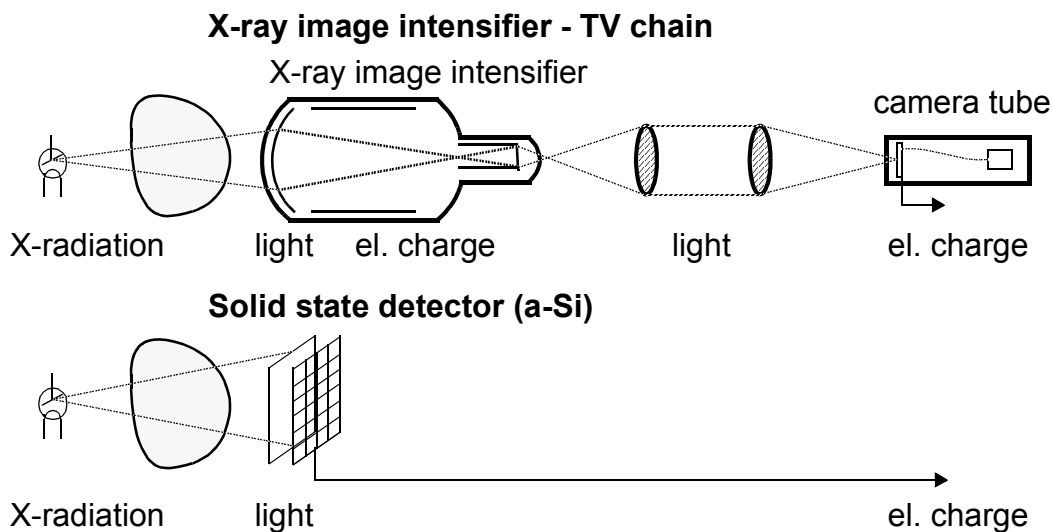


**Figure 1:** Comparison between XRII-TV chain and a-Si solid state detector

Hence, the requirements to realize an a-Si X-ray detector are a large area scintillator and a large area photoconductor. Optimal performance is obtained by CsI doped with TI, and plasma-deposited hydrogenated amorphous silicon which can be both easily deposited on the required areas of human body dimensions.

The well-known advantages of a-Si are its low deposition temperature which enables the use of nearly arbitrary substrates, its ample semiconductor properties (photoconductivity, field effect), its compatibility with silicon process technology, and of course its good stability against X-ray radiation.

The disadvantage of restricted stability against prolonged illumination (Staebler-Wronski effect) is not disturbing since the photodiodes are operated under reverse bias and the light intensities are several orders of magnitude lower than those applied to solar cells.

## 2. Detector Design and Technology

The detector consists of a 450  $\mu\text{m}$  thick CsI:TI layer coupled to the a-Si panel (Fig.2). A matrix of 1024  $\times$  1024 pixels  $196 \times 196 \mu\text{m}^2$  in size is built on a glass substrate. Each pixel is connected to a column line for readout and a row

line to apply driving voltages. Optical reset light flashes can be applied from the bottom of the photodiodes through the substrate. The detector is completed by driving and readout electronics, analog-to-digital converters, a programmable timing generator, and a system board with optical fibre communication to the host computer.

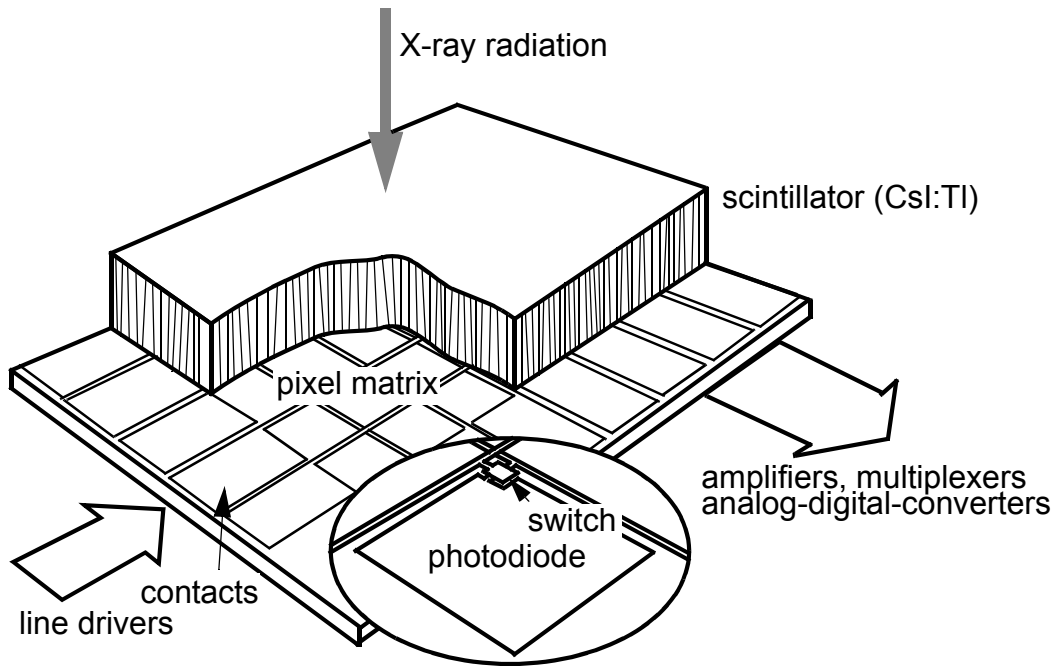


**Figure 2:** Schematic drawing of an a-Si X-ray detector panel

Every pixel consists of a NIP photodiode and a PIN switching diode (Fig.3). Compared to using thin-film transistors (TFTs), this double diode technology is easier to produce and has the advantage of a better fill factor. The fill factor is the percentage of photodiode area with respect to the pixel area, in our case 70%.

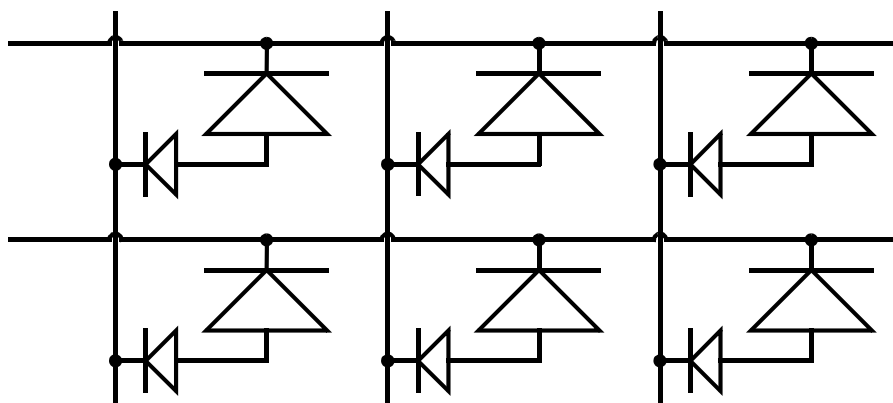


**Figure 3:** Pixel structure of the double diode technology. The row lines are for driving voltage pulses, the column lines are for charge readout

The diodes are made from hydrogenated a-Si deposited by a conventional plasma-enhanced CVD process. The photodiodes are optimized for low dark current ( $< 1 \text{ nA/cm}^2$  at  $-4 \text{ V}$ ) and high quantum efficiency in the visible spectral range ( $> 80\%$  at  $550 \text{ nm}$ ). The capacity of one photodiode is  $1.9 \text{ pF}$ .

The switching diodes are very small ( $20 \times 20 \text{ }\mu\text{m}^2$ ). Their leakage current is  $10 \text{ nA/cm}^2$  at  $-4 \text{ V}$ . To enable high forward currents, they exhibit an ideality factor  $n_s = 1.8$  and a low series resistance.

The timing diagram of one frame is depicted in Fig. 4: a first voltage pulse VP1 (typically  $\approx 4 \text{ V}$ ) is applied to all photodiodes of the whole panel simultaneously and biases them in reverse.

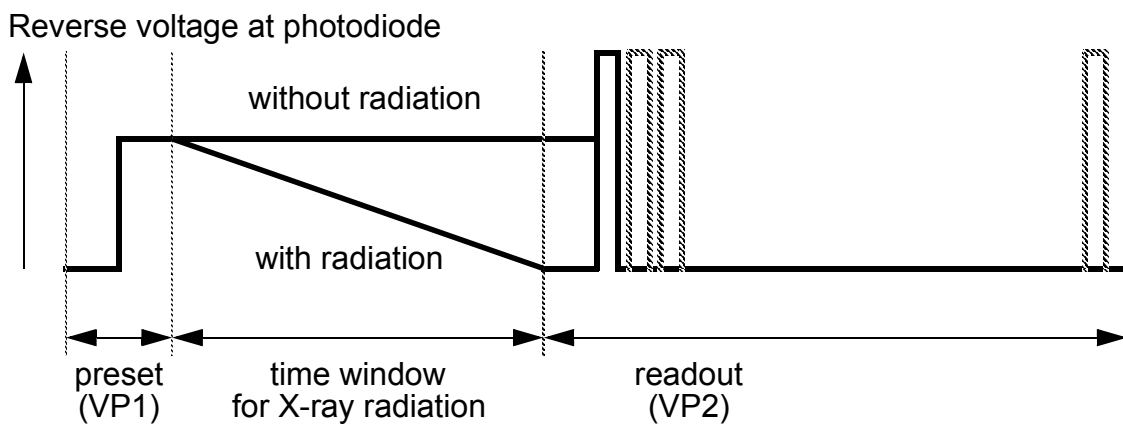


**Figure 4:** Frame timing of the double diode detector panel. The reset light is included in the preset phase

Then a time interval of several milliseconds is retained where the X-ray tube can be switched on. Depending on the local dose incident on the detector, light and accordingly charges are generated in the photodiodes resulting in a voltage drop.

Subsequently, a second voltage pulse VP2 ( $\approx 4.5 \text{ V}$ ) is applied row by row, charging the diodes to a somewhat higher voltage. The charge needed is read out via the column lines and fed to a custom designed readout amplifier. This charge is a measure for the X-ray intensity.

The final step is a short back-side illumination of the panel. This reset light flash discharges all diodes and fills the deep traps in the a-Si to ensure equal starting conditions for all diodes in the next frame. The reset light intensity has to be optimized carefully to guarantee a trap occupancy which is able to reduce the memory effect (see below) markedly.

A difficulty occurs because it is impossible to charge a capacitor in a short time through a diode like in the case of a resistor. No exponential behaviour with a fixed RC time constant is observed, but a much slower course. This leads to a poor linearity at low signals. Reproducible results can only be obtained with a

voltage pulse  $VP2 > VP1$  which results in an additional offset charge. This charge is subtracted later on during the correction procedure.

The readout circuits have 120 charge sensitive input channels with several switchable sensitivity ranges, sample-and-hold circuits, and an output multiplexer. After amplification, the signal is digitized with 12 bit resolution. A fast image processor (input data rate  $> 25$  MB/s) enables subtraction of dark images, correction of individual pixel gain, and repair of defective pixels by interpolation from their neighbour pixels in real-time.

### 3. Detector Performance

The detector is operated basically in two different modes: fluoroscopy to examine the patient in real-time for a longer time, and radiography to take single images. In fluoroscopy a very low X-ray dose is necessary. Typical system dose, i.e. the average dose over a region of interest, is 15 nGy per image with a frame rate of 12.5 Hz ( $1024 \times 1024$  matrix) or 25 Hz ( $512 \times 512$  matrix). The system dose for radiography is in the order of  $\approx 1$   $\mu$ Gy.

The detector sensitivity (= the number of electrons which are read out per X-ray quantum incident on the detector surface) is  $1150 e^-/X_{inc}$ . This value is equivalent to a photo-electric sensitivity (= the number of electrons which are generated on the photodiode area per X-ray quantum absorbed on this area in the scintillator) of  $2400 e^-/X_{abs}$ . Measuring conditions were 70 kV tube voltage and 21 mm aluminium beam filtration<sup>6</sup>. This leads to an X-ray spectrum which is similar to the one used in standard medical investigations.

Key parameters for image quality are the DQE, the spatial resolution expressed by the modulation transfer function (MTF), linearity, image lag, coarse contrast ratio, and long term stability. The DQE is the most important quantity to characterize X-ray detectors since it is a measure for contrast detail detectability and dose requirement. Beside X-ray absorption, electronic noise contributions determine the DQE at low dose.

Fig.5 shows the dependence of the DQE on spatial frequency for different doses. In the case of radiography (high dose), signal and quantum noise are large compared to the electronic noise. Thus the DQE at low spatial frequencies reaches the value of X-ray absorption which is around 70%.

With lower dose, the DQE decreases markedly. That means that the image quality is reduced by electronic noise. Accordingly, fluoroscopy is the most demanding mode for the a-Si detector.

Therefore, special emphasis has been laid on the origin of the different noise sources. The total electronic noise level with respect to the a-Si panel output amounts to  $1450 e^-$ . This noise is composed of the following contributions:

- pixel noise which comes from the photodiode reset and amounts to  $\approx 750 e^-$  ( $\sqrt{n_s k T C_p}$  depending on the photodiode capacitance  $C_p$  and the switching diode ideality factor  $n_s$ )

- shot noise originating from leakage currents ( $< 250 e^-$ )
- emission from traps ( $\approx 400 e^-$ )
- the readout circuits in use today deliver a noise of  $\approx 10^{10} e^-$  operated with an input load of 115 pF
- minor noise sources are line resistances, analog chain, and the AD converter

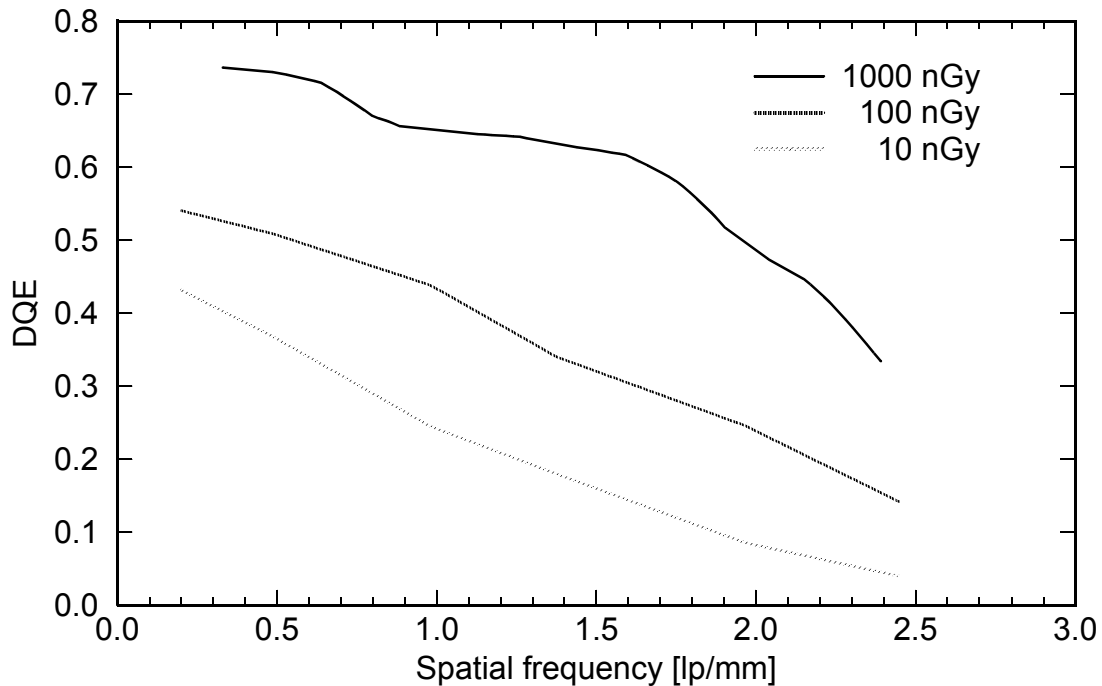


**Figure 5:** DQE of the a-Si detector at different doses

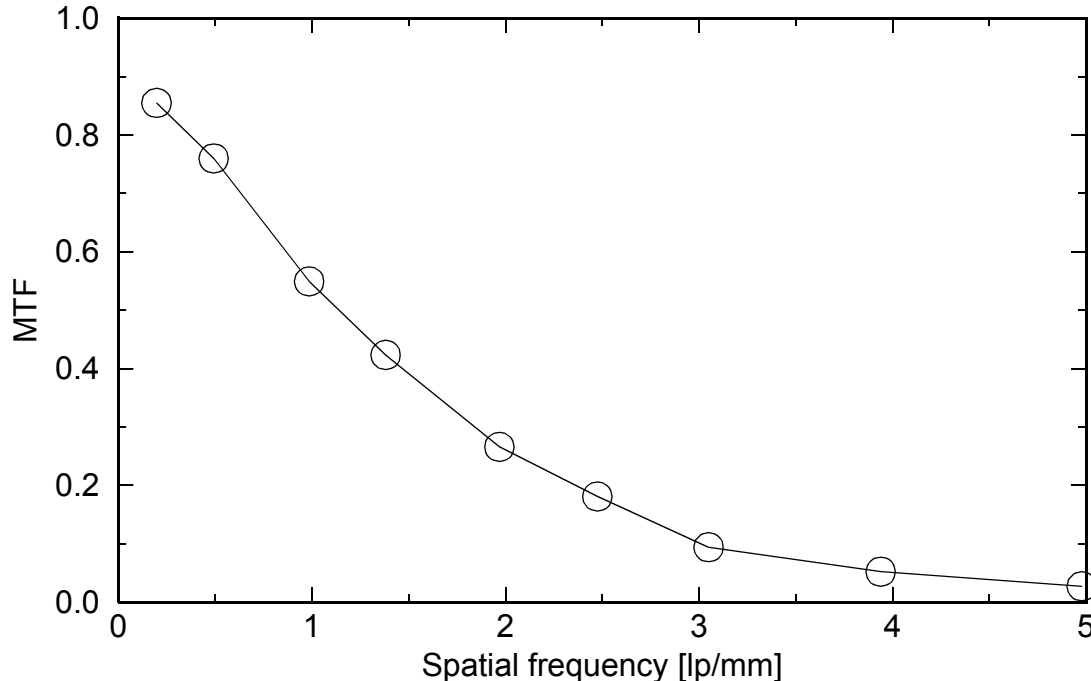
MTF is beside DQE crucial for small detail detectability. It is determined by the spatial resolution of the scintillator and the size of the photodiodes. The light output of the CsI layer is enhanced by a white reflector on the back side which however deteriorates resolution.

Fig.6 shows the MTF of the detector with 196  $\mu\text{m}$  pixel pitch. It should be pointed out that even near the Nyquist frequency which is 2.55 line pairs per mm for this type of detector, the MTF is still 18%. As a matter of fact, this good MTF can lead to aliasing effects.

Since the photodiodes are operated under reverse bias, the photocurrents are of primary nature<sup>7</sup>. Therefore, a good linearity behaviour is expected. At -4 V, errors of 0.3% were observed. Other linearity aberrations in the order of  $\approx 1\%$  originate from the readout circuits.

The time response behaviour of the detector is crucial for practical applications. Single images must not show ghost images of former investigations. Real-time fluoroscopy must be free from image lag. This is particularly crucial when high dose images were taken shortly before. The amplitude of a residual image in the following frame is  $< 3\%$  under most circumstances. The origin of this lag is

mainly deep trapping and emission of electrons from traps in the a-Si diodes<sup>8</sup>. But CsI:TI is also known to show some afterglow. This topic is currently under investigation.



**Figure 6:** MTF of the a-Si detector

The coarse contrast ratio is the image signal ratio between the maximum signal and the signal behind a large area of a totally absorbing object (e.g. a lead disk). Values of > 1:100 are reached which are markedly larger than those of the XRII-TV chain ( $\approx 1:20 - 30$ ).

Long term stability of the a-Si detector seems to be no major problem. After application of a lifetime X-ray dose ( $\approx 80$  Gy), only a slight increase in dark offset was observed. Since the offset is acquired permanently during stand-by, such an increase or little drifts due to temperature changes are subtracted automatically.

#### 4. Conclusions

The a-Si detector exhibits all properties which are required for medical X-ray diagnosis. Therefore, a sample of our detector has been tested in a clinical site for more than one year. Over 200 patients have undergone cardiac investigations. The results demonstrate the outstanding image quality especially at higher dose (digital cinema mode).

On the other hand, the signal-to-noise ratio at low dose (fluoroscopy) still has to be improved. This can be accomplished by advanced design rules for the a-Si panel itself, improved process technology, and the next generation of read-out circuits.

In summary, the following advantages of the a-Si detector should be pointed out:

- flatness and compactness, lighter and more handy system
- no geometrical distortions (neither due to magnetic fields nor at the edges)
- homogeneous resolution and sensitivity over the whole image area
- excellent large area (coarse) contrast, compared to XRII-TV systems
- high sensitivity and thus, possible dose reduction
- real-time radiography (no film processing, no cassette handling)
- no optics, no vacuum, no chemicals
- direct image transfer to PACS (Picture Archiving and Communication System)
- mixed fluoroscopic and radiographic applications with one system feasible

Our work has furnished evidence for the usefulness of the detector concept and the excellent performance. Hence, a first milestone was reached towards the goal of replacing existing fluoroscopic (XRII-TV) and radiographic (storage phosphor) systems for medical diagnosis.

## 5. References

- [1] U. Neitzel, I. Maack, S. Günther-Kohfahl, *Med. Phys.* **21**, 509, 1994
- [2] J. Chabbal, C. Chaussat, T. Ducourant, L. Fritsch, J. Michailos, V. Spinnler, G. Vieux, M. Arques, G. Hahm, M. Hoheisel, H. Horbaschek, R. Schulz, M. Spahn, *Proc. of SPIE 2708 Physics of Medical Imaging*, 499, 1996
- [3] T. Graeve, Y. Li, A. Fabans, W. Huang, *Proc. of SPIE 2708 Physics of Medical Imaging*, 494, 1996
- [4] U. Schiebel, N. Conrads, N. Jung, M. Weibrecht, H. Wieczorek, T. Zaengel, M. J. Powell, I. D. French, C. Glasse, *Proc. of SPIE 2163 Physics of Medical Imaging*, 129, 1994
- [5] L. E. Antonuk, J. Yorkston, W. Huang, J. Boudry, E. J. Morton, R. A. Street, *Proc. of SPIE 1896 Physics of Medical Imaging*, 18, 1993
- [6] equivalent to DN5 defined in German Standard DIN6872
- [7] M. Hoheisel, G. Brunst, H. Wieczorek, *J. Non-Cryst. Solids* **90**, 243, 1987
- [8] H. Wieczorek, *J. Non-Cryst. Solids* **164-166**, 781, 1993

## 6. Acknowledgements

The project was also advanced by numerous co-workers at Thomson Tubes Electroniques. The contributions of D. Hassler, G. Schmidt, H. Schreiner, K. Stierstorfer and many others of Siemens Medical Engineering are gratefully acknowledged.

This work was supported in part by EUREKA grant EU 651 under the name ASTRID (Amorphous Silicon Technology for Radiographic Image Diagnostic) and by the French Department of Industry.

